a = catalyst pellet size (diameter), cm.
D = diffusivity, sq.cm./sec.; D_K = Knudsen diffusion coefficient; D_B = ordinary diffusion coefficient in the bulk gas phase
D_e = effective diffusivity, usually $\chi\epsilon D_B$ or $\chi\epsilon D_K$
E = effectiveness factor
E_o = activation energy in Arrhenius equation
F = flow rate of feed to reactor, cc. at reactor temperature and pressure/sec.
F_s = fractional activity of selectively poisoned catalyst
f = any functional relationship
G = superficial mass velocity, g./sq.cm.sec.
h = Thiele parameter, dimensionless
h_o = Thiele parameter for unpoisoned catalyst; h and h_o can be used interchangeably where poisoning is not a factor
k_g = intrinsic reaction velocity constant, cc. fluid volume/sec./g. of catalyst
k_{gs} = experimentally measured reactivity, same units as k_g
P = pressure
R_g = gas constant, 82.06 cc. atm./g. mole °K.
r = pore radius, usually 2 V_g/S_g, cm.
S_g = specific total catalyst surface area, sq.cm./g.
S_e = external surface area of one catalyst pellet, sq. cm.
T = absolute temperature
V_g = specific internal void (pore) volume, cc./g.
V_p = volume of one catalyst pellet, cc.
W = weight of catalyst in bed, g.
x = moles of cyclohexane converted to benzene per mole of cyclohexane fed
Y = function of x defined by Equation (6), dimensionless

Greek Letters

α = fraction of catalyst surface which is poisoned, dimensionless
ϵ = porosity within a single catalyst pellet, dimensionless
μ = viscosity, g./cm.sec.
ρ = gas density, g./cc.
ρ_p = pellet density of catalyst, g./cc.
χ = tortuosity factor defined above, see D_e

LITERATURE CITED

1. American Documentation Institute, Photoduplication Service, Library of Congress, Washington 25, D. C., document No. 6528, may be obtained for $1.25 for photoprints or for 35-mm. microfilm.
2. Bar-Ilan, Mosche, and William Resnick, *Ind. Eng. Chem.*, **49**, 313 (1957).
3. Brown, G. G., *et al.*, "Unit Operations," p. 79, Wiley, New York (1950).
4. Hoogschagen, Jan., *Ind. Eng. Chem.*, **47**, 906 (1955).
5. Kettenring, K. N., E. L. Manderfield, and J. M. Smith, *Chem. Eng. Progr.*, **46**, 139 (1950).
6. Kivnick, Arnold, and A. N. Hixson, *ibid.*, **48**, 394 (1952).
7. Mathis, J. F., and C. C. Watson, *A.I.Ch.E. Journal*, **2**, 518 (1956).
8. Petersen, E. E., *ibid.*, **3**, 443 (1957).
9. *Ibid.*, **4**, 343 (1958).
10. Resnick, William, and R. R. White, *Chem. Eng. Progr.*, **45**, 377 (1949).
11. Shen, C. Y., and H. F. Johnstone, *A.I.Ch.E. Journal*, **3**, 349 (1955).
12. Thiele, E. W., *Ind. Eng. Chem., Analyt. Edit.*, **31**, 916 (1939).
13. Wagner, C. P., *Z. physik. Chem.*, **A193**, 1 (1943).
14. Weisz, P. B., and C. D. Prator, "Advances in Catalysis," Vol. 6, pp. 143-196, Academic Press, New York (1954).
15. Weisz, P. B., and E. W. Swegler, *J. Phys. Chem.*, **59**, 823 (1955).
16. Wheeler, Ahlborn, "Advances in Catalysis," Vol. 3, pp. 250-326, Academic press, New York (1950).
17. ———, "Catalysis," Vol. 2, pp. 105-165, Reinhold, New York (1955).
18. Wilke, C. R., and C. Y. Lee, *Ind. Eng. Chem.*, **47**, 1253 (1955).
19. Zeldowitch, J. B., *Acta Phisiochem., USSR*, **10**, 583 (1939).

Manuscript received July 21, 1959; revision received May 6, 1960; paper accepted May 6, 1960. Paper presented at A.I.Ch.E. Kansas City meeting.

Mass Transfer with Liquid Lithium in Circular Conduits

WILLIAM N. GILL, RICHARD P. VANEK, and C. S. GROVE, JR.

Syracuse University, Syracuse, New York

Forced convection mass transfer between circular tubes and liquid lithium was experimentally investigated over a range of Schmidt numbers from 40 to 57 and Reynolds numbers from 5,550 to 22,500. *Information concerning the mechanism for mass transfer was obtained by measuring* local solution and deposition rates as a function of distance along the tubes. Observed entrance effects for the solution process suggest that it involves the parallel mechanisms of diffusion through a solid film and through occluded liquid in grain boundaries. It is indicated that the relative contributions of these processes changes with increasing temperature.

A j-factor correlation of existing liquid metal mass transfer data for fully developed conditions in circular conduits is presented and indicates that an exponent of 0.112 for N_{Re} best represents the data. This result agrees well with other studies (9).

A number of quantitative studies of mass transfer between turbulent flowing fluids and circular conduits have been made for the purpose of testing and extending the existing theories of mass transfer and also to provide correlations satisfactory for design pur-

poses. Several investigations utilized the falling film column and obtained data for a wide range of Reynolds numbers with Schmidt numbers generally varying between 0.5 and 15 (*17*). Data for the transfer of solid organic compounds to water have been obtained at various Reynolds numbers and at Schmidt numbers from 1,000 to 3,000 (*15*). The results of a study of mass transfer from zinc tubes to flowing mercury have been reported for Schmidt numbers varying between 82.5 and 83.9 (*7*).

Very few quantitative data concerning mass transfer in alkali metal systems are available. Solution rate constants for liquid sodium systems have been reported (*8, 12*), and mass transfer coefficients and solution rate constants for the turbulent boundary-layer flow of liquid lithium along flat plates are available (*10*). Mass transfer coefficients for liquid alkali metals flowing in circular tubes are apparently not available either in the entrance section or with fully developed conditions.

APPARATUS AND PROCEDURE

An experimental apparatus similar to that employed here has been described previously (*10*) with the exception of the test sections, which were designed to measure entrance and fully developed mass transfer rates and coefficients. The solution and deposition sample sections were constructed similarly. For each test section fifteen Type 304 ½-in. O.D. stainless steel tubular specimens were carefully machined to form a smooth continuous tube 27 in. long, electropolished to remove surface irregularities and films and weighed on an analytical balance. The sample tube was then inserted into a ⅝-in. O.D. supporting tube, which was slotted lengthwise to facilitate solution of the solid lithium between the concentric tubes after removal of the test section from the system. The nominal ⅝-in. supporting tube containing the specimens was then inserted into a ¾-in. tube and the entire assembly fitted on each end with connectors machined to hold the three tubes concentrically. Since the entire system was made of Type 304 stainless steel, both the hydrodynamic and diffusion boundary layers would be fully developed at the entrance to the test section. Therefore to investigate the effect of boundary layer formation, which in turn provides information concerning the transfer mechanism, it was necessary to have a sharp edged entrance providing an approximate uniform initial velocity and concentration distribution.

Lithium in the charge tank was melted and forced by argon pressure through a 5-μ pore size stainless steel filter into the loop system. Sufficient lithium was added in the initial charge so that the loss in each of the removed sample sections would not seriously affect the lithium level in the surge tank. Pumping, flow metering, temperature control, and filtration were as previously described (*10*). Continuous filtration during the entire cooling process effected an extremely low level of contamination. The effectiveness of the procedures employed for the reduction of contamination is indicated by the results of oxygen and nitrogen analyses performed on lithium taken from the system:

Lithium analysis

O_2	—	2.2 p.p.m.
N_2	—	190 p.p.m.

The oxygen concentration reported is the average of three duplicate analyses, and the nitrogen value is the average of two analyses. These analyses indicate that the lithium used was very pure, and the results obtained would not be applicable to contaminated systems.

After the series of runs with tubular samples was made, a qualitative run was performed with flat plate nickel specimens arranged in sample sections similar to those used previously (*10*). Plugging of the loop occurred after 70 hr. of operation, and the run was terminated. The samples were then removed and inspected; however, only qualitative information could be obtained owing to the severe attack.

RESULTS AND DISCUSSION

Since mass fluxes may be measured with relatively little difficulty, it is convenient to obtain bulk mean liquid concentration differences from observed fluxes with the continuity equation in the form

$$C(x) - C(O) = \frac{A_p}{A_c\, U_{avg}} \int_o^x N_o dx \qquad (1)$$

Consequently if the bulk mean liquid concentration is known at any point in the system, and fluxes from the wall to the liquid are measured around the system, then the concentration at any other point can be determined by using Equation (1). The system under consideration was particularly amenable to this procedure, since the transfer area around the entire system was well defined.

In nonisothermal dynamic loop systems the solution process is complicated and not well understood. Some disagreement exists concerning the rate determining process for the solution of iron in sodium (*8, 12*) which was attributed to discrepancies in the solubility data used. Horsley (*12*) concluded that transfer rates observed were generally larger than those calculated on the basis of a diffusion limited mechanism. However his calculations were based on a correlation for fully developed conditions in tubes and the solubility data used were for pure iron, whereas the observed rates were reported for Society of Automotive Engineers 1020 steel and the hydrodynamic conditions were not well defined and probably involved developing momentum and diffusion boundary layers. Either of these conditions could account for the differences reported. Because of the uncertainties involved the solution rate is generally described linearly in terms of an over-all coefficient (solution rate constant) and an over-all driving force equal to the difference between the equilibrium and bulk mean concentrations. Hence

$$N_o = \alpha\ \Delta C \qquad (2)$$

where ΔC for any point x in the system is from Equation (1)

$$\Delta C = C^\circ(x) - C(x) = C^\circ(x) - \left[C^\circ_f + \frac{A_p}{A_c\, U} \int_o^x N_o\, dx\right] \qquad (3)$$

and N_o in Equation (3) is known from measurements around the system.

To determine the correct values of equilibrium concentrations to be used in Equation (3) it is necessary to know which elements or metals are transferring and the solubility of these materials in liquid lithium. The major constituents of Type 304 stainless steel are nickel, chromium, and iron; manganese, silicon, and carbon are also present but in much smaller quantities. Since the surface area of the system including the filter pores is extremely large, the filter outlet concentration, C°_f, may be considered to include all major components in equilibrium amounts. Therefore $C^\circ(x)$ should logically include the solubilities of iron, nickel, chromium and α will therefore reflect the total resistance to transfer. Since the solubility of nickel is much greater than that of iron and chromium, the value of α will be dominated by the nickel solubility.

It has previously been shown (*10, 11*) that iron, nickel, and chromium are all transferred to some extent in austenitic stainless steel systems. Spectrographic analysis of cold trapped crystals and x-ray analysis of specimens in the high and low temperature sections confirmed those reported previously (*10*). The cold trapping method used to obtain crystals for spectrographic analysis is strongly biased in favor of obtaining nickel crystals because nickel solubility changes with temperature are very large compared with those of iron and chromium. However the progressively increasing austenite to ferrite formation with increasing temperature shown by x-ray analysis strongly indicate preferential nickel loss which was also observed by Hoffman and Trotter (*11*). Chemical analysis of products

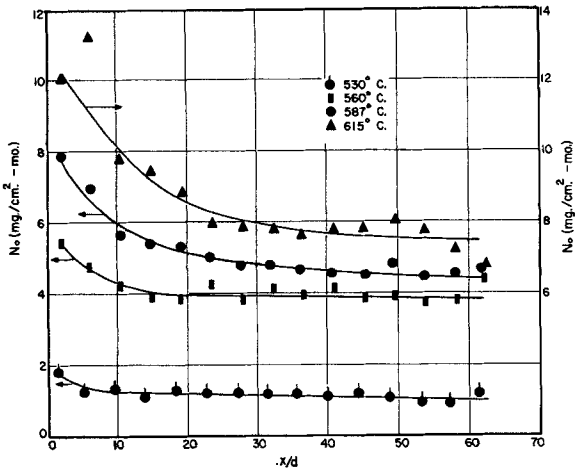

Fig. 1. Local solution rate vs. x/d.

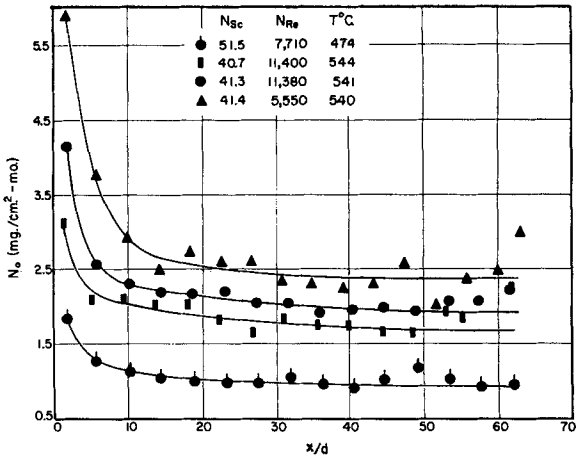

Fig. 3. Local deposition rate vs. x/d.

on deposition section specimens to a depth of 0.006 in. showed 99.85% iron, chromium, nickel in the first 0.003-in. increment with a decrease to 98.77% in the next, and the individual percentages of all components decreased with increasing distance from the surface. The accumulated results of chemical, spectrographic, and x-ray analyses performed indicate that all components were transferred but that nickel transferred preferentially; however the exact extent could not be precisely determined.

Solubility data for iron, chromium, and nickel are now available from several studies (*1, 3, 13, 18*). The data of Leavenworth, Smith, and Cleary (*13*) are most consistent, and heats of solution determined from these data agree well with the theoretical predictions of Strauss, Brown, and White (*19*). It might be mentioned that Bagley and Montgomery's (*1*) solubility data agree reasonably well with those of Leavenworth et al., despite the fact that they used Type 304 stainless steel rather than pure nickel. This strongly indicates that little error is introduced by assuming the iron, chromium, and nickel of the steel act as they would independently regarding equilibrium solubility. With $C°$ in parts per million

$$\ln C°_{Fe} = = 9.55 - \frac{5{,}960}{T}$$

$$\ln C°_{Ni} = = 7.805 - \frac{3{,}960}{T}$$

$$\ln C°_{Cr} = = 15.08 - \frac{7{,}530}{T}$$

When one assumes saturation at the filter outlet, the driving force for deposition is the difference between the supersaturated bulk mean concentration and the interfacial concentration which is identical to the difference between the supersaturated bulk mean concentration and the filter outlet concentration. It is particularly important that this concentration difference can be determined from direct measurements on the system by the use of Equation (1) and is independent of solubility data or an assumed mechanism for the solution process. When one uses this concentration difference, the mass transfer coefficients are calculated by

$$k = \frac{N_o}{\Delta C} \qquad (4)$$

No data are available for values of the diffusivities of nickel, chromium, and iron in liquid lithium, but it has been shown (*10*) that the Stokes-Einstein equation

$$\frac{D\mu}{T} = \frac{K}{6\pi R_A} \qquad (5)$$

may be used to determine diffusivities with sufficient accuracy for mass transfer calculations. Since values of the atomic radii for these three metals differ only slightly, an average value may be used.

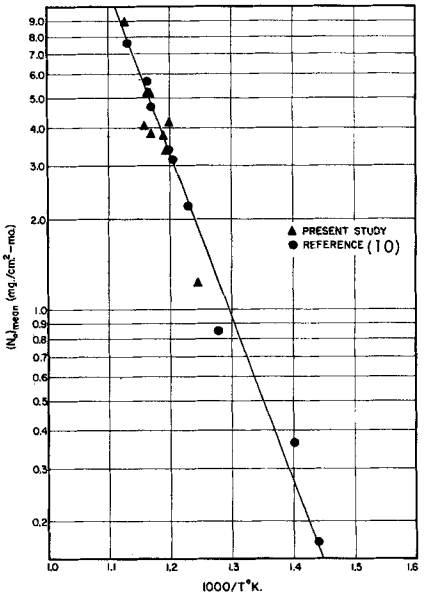

Fig. 2. Variation of mass flux with temperature.

Solution Data

Local solution rates were measured, as shown in Figure 1, for a substantially uniform entrance velocity and concentration distribution, since a sharp edged entrance was provided. The most interesting aspect of these curves is the curvature of the lines which is most pronounced at x/d less than 30 for all of the curves. Since the over-all driving force is essentially constant for a given curve, and if the rate-controlling mechanism was the solid solution process, it would be expected that little or no curvature would exist and the rate would be almost constant exhibiting a very slight decrease as x/d increased. The observed curvature, which increases with temperature, indicates that the mass flux is not entirely controlled by solid-phase effects, but is also affected by the fluid dynamics of the system, since boundary-layer formation along the tube is evident. Consequently as the temperature of the lithium increases, the effect of liquid-phase diffusion resistance increases, and it would seem desirable to examine how this may occur.

Initially all components may be assumed to be in equilibrium at the surface, and grain boundary penetration is negligible. At this time liquid-phase convective diffusion would control the transfer of all components. Because of its much higher solubility nickel depletes most rapidly in the solid surface layers and must be replaced by solid-phase diffusion which restricts its rate of solution markedly. If this process continued uninterrupted, the solution rate would eventually be controlled by diffusion of iron because of favorable solid-phase gradients, and the over-all rate of solution would be much higher than those observed without any assistance from grain boundary effects as

TABLE 1. EXPERIMENTAL CONDITIONS

T_S, °C.	T_D, °C.	Time, (hr.)	$(N_{Re})_D$	$(N_{Sc})_D$	$\Delta C_D \times 10^5$ (mg./cc.)	$J_D \times 10^3$	ΔC_S,* (mg./cc.)	$\alpha_m \times 10^6$,* (cm./sec.)	$\left(\frac{N_{calc}}{N_{obs}}\right)_{Fe}$	$\left(\frac{N_{calc}}{N_{obs}}\right)_{Cr}$	$\left(\frac{N_{calc}}{N_{obs}}\right)_{Ni}$
448	432	200	22,500	60.8	0.27	3.65					
566	544	100	14,500	40.6	3.51	4.01	0.047	25.4	21.0	23.3	950
564	540	100	12,200	42.1	3.81	3.80	0.0540	24.1	14.8	21.6	850
589	544	55	11,410	40.6	5.0	2.70	0.114	13.65	28.5	36.4	1510
587	541	100	11,380	41.3	4.8	3.26	0.110	18.3	18.3	22.9	905
560	521	100	9,620	43.9	2.82	3.20	0.076	21.0	16.9	23.2	800
530	474	100	7,700	51.5	2.54	4.87	0.076	6.2	50.0	79.2	2160
580	550	100	7,000	40.8	8.6	4.4	0.072	20.3	12.4	17.6	632
615	540	100	5,550	41.4	12.9	3.2	0.195	17.6	12.8	14.6	642
585	450	100	4,000	56.6	7.8	4.8	0.217	9.22	20.0	28.2	875

* Based on combined solubility of iron, nickel, chromium.

seen in Table 1. It therefore must be assumed that an inhibitive process of some kind occurs at the surface, possibly similar to that described by Epstein (*8*) for stainless steel-sodium systems. Static tests at 500°C. for austenitic stainless steels in lithium indicated weight increases of the specimens which may be attributable to the formation of such a film through which the constituents must diffuse. The results shown in Figure 1 however indicate that other processes influenced by the hydrodynamic conditions must necessarily occur as well, since it is rather unlikely that a film protected surface would be so markedly influenced unless the surface was not completely covered. These effects probably occur at high energy grain boundaries. Consider the interstices between grains with lithium advancing along the boundary by dissolving interstitial material which is characterized by an excess free energy over that in the grains (*16*). As this takes place, additional surface area is made available for solution. Small degrees of penetration create rather large interstitial surface area to liquid volume ratios, and it is likely that this occluded liquid is much closer to saturation in all components than the film protected solid-liquid interface. Each component would therefore be removed from the pore entrance in proportion to its solubility, and consequently nickel would be expected to be removed preferentially owing to its high relative solubility. At very high temperatures grain boundaries could be depleted sufficiently to cause the removal of grains in particulate form as has been observed in high temperature thermal convection loops (*11*). Since entrance effects for the solution process are observed to be less pronounced than for the deposition process, it is probable that both solution and diffusion limited mechanisms significantly contribute to the over-all transfer and act in parallel in the temperature region investigated. Table 1 includes values of α based on the combined solubility of iron, chromium, and nickel and the initial internal surface area of the tube. It should be noted that these α's are particularly misleading if used for mechanism considerations. If transport is through the protective film in the steady state, it would be predominantly due to the solution of iron because of favorable solid phase gradient behind the film; also the transfer of nickel or other components along grain boundaries is based on much smaller contact area with the bulk stream than that used in the calculation of α. Therefore regardless of the mechanism it would not be reflected in the magnitude of α. Also included are ratios of fully developed solution rates of iron, chromium, and nickel calculated for a diffusion limited mechanism with Equation (7) to the observed rates given in Figure 2. Although the values scatter substantially, they show a statistically significant tendency to decrease with increasing temperature and further indicate a transition in the transport mechanism. This transition is probably caused by the large temperature coefficients characteristic of solid-phase diffusion processes; in addition intergranular excess free energy considerations show that both the rate of penetration and the interstitial solubilities are increased as well. An approximate expression given by Horsley (*12*) indicates that the difference between grain boundary and normal saturation in lithium increases to a maximum well above the temperatures investigated here. This difference is most pronounced for nickel because of its higher heat of solution as seen in the previously given solubility expressions. The average rates of solution for various experimental conditions are presented in Figure 2. These data compare very favorably with those obtained for solution from flat plates and further confirm that the average solution rate may be adequately represented as an exponential function of temperature.

Deposition Data

Local deposition rates are presented in Figure 3. These data exhibit stronger curvature in the region $0 \leq x/d \leq 20$ than observed in the solution process. A marked decrease in curvature for this family of curves is noted at $x/d > 20$. The entrance condition was essentially a uniform velocity and concentration distribution, and therefore the development of the momentum and diffusion boundary layers must both be considered. Deissler (*6*) has observed that the velocity distribution for flow in a tube with a right-angle entrance at a point relatively close to the wall is fully developed at an x/d of 25. This value corresponds well with the present data which indicate that the diffusion boundary-layer formation is essentially complete at x/d between 8 and 20, depending on the conditions. With Schmidt numbers on the order of 40 to 50 the major part of the radial concentration change takes place relatively close to the wall. Therefore it would be expected that the diffusion boundary layer would be substantially developed at x/d less than that required to establish the hydrodynamic boundary layer. In particular the diffusion boundary layer in this case should be substantially developed closer to the wall than the above mentioned measurements of Deissler. Linton and Sherwood (*15*) obtained limiting mass transfer rates at an x/d on the order of 6 for N_{Sc} between 1,000 and 3,000. It would obviously be expected that fully developed conditions would be obtained at larger x/d for lower N_{Sc} values. The fact that the deposition curves exhibit greater curvature than the solution curves suggests that the deposition process is principally dependent upon liquid-phase diffusion and the rate is probably diffusion limited. The mass transfer coefficients discussed below also substantiate this conclusion.

Mass Transfer Coefficients

Mass transfer correlations proposed by various investigators are generally of the form

$$\frac{k}{U_{avg}} \phi_D = f/2 \qquad (6)$$

where ϕ_D is a function of N_{Sc} and other dimensionless parameters of the sys-

tem. Correlations of this type have been proposed by Sherwood (17), Boelter et al. (2), Lin et al. (14), Chilton and Colburn (4), Deissler (5), and others. The simplest and perhaps most widely used is that of Chilton and Colburn which has been compared with the present data and those obtained by Dunn et al. (7) in Figure 4. Since the data scatter some, it is difficult to determine how good the agreement is; however the sixteen points shown are sufficient to obtain meaningful information from a least-square analysis which yielded the following relationship:

$$j_D = 0.01\ N_{Re}^{-0.112} \qquad (7)$$

This equation has been plotted in Figure 4 for comparison. Friend and Metzner (9) have discussed the N_{Re} exponents obtained from heat transfer studies at high N_{Pr}, and on this basis it appears that the exponent in Equation (7) agrees well with other investigations. Furthermore it is seen that the Chilton-Colburn analogy in which ϕ_D is taken as $N_{Sc}^{2/3}$ agrees reasonably well with the experimental values, and considering the uncertainties involved concerning the physical constants used it does not seem realistic to compare these data with other more refined analogies. However the agreement obtained is certainly adequate for design purposes.

CONCLUSIONS

1. Measurements of solution rates in the entrance to circular tubes indicate that mass transfer to the liquid stream is significantly influenced by hydrodynamic conditions and suggest that the solution process involves transfer along grain boundaries and through a protective film, both of which are strongly influenced by temperature. The former is attributable to the excess free energy of grain boundary material which enhances its solubility. A comparison of calculated and observed rates for fully developed conditions supports this conclusion.

2. The deposition data support the previous observation (10) that the deposition process is limited by liquid-phase diffusion, and therefore mass transfer coefficients may be determined with conventional correlations.

3. Investigation of solid-liquid systems in which the solid exhibits a low solubility in the liquid offer several advantages for the study of fundamental mass transfer concepts and the testing of proposed theories. The greater share of the correlations, as proposed in the literature, are derived with the assumption that the mass fluxes are not of sufficient magnitude to affect the velocity distribution, and these systems can be designed to closely approximate such conditions. Also the simultaneous study of solution and deposition phenomena is important in determining the transport mechanism which may be controlled differently in each case.

4. The values of mass transfer coefficients obtained in this study cannot be explained by the assumption of a completely laminar sublayer and further support the assumption that turbulence exists up to the wall.

5. The use of pure nickel as a container for liquid lithium is not advisable owing to the extreme corrosion rates encountered at elevated temperatures. The high transfer rates are due to the relatively high solubility of nickel in liquid lithium and indicate that the solution process for pure nickel is diffusion limited.

ACKNOWLEDGMENT

This investigation was sponsored by The National Science Foundation under Grant G-5085. Some equipment was supplied by M.S.A. Research and The Crawford Fitting Company and is gratefully acknowledged. The authors are also grateful to the Oak Ridge National Laboratory for performing the oxygen and nitrogen analyses.

NOTATION

A = area, (L^2)
C = solute concentration, (M/L^3)
d = diameter, (L)
D = molecular diffusivity, (L^2/θ)
f = Fanning friction factor
k = mass transfer coefficient, (L/θ)
N_o = mass flux at the wall, (mg./sq. cm. sec.)
R_A = atomic radius, (Å.)
T = temperature, (°K.)
U_{avg} = average velocity, (cm./sec.)
x = distance from the origin (L)
j_D = Chilton-Colburn j factor, $(k/U_{avg})\ Sc^{2/3}$

Dimensionless Groups

N_{Re} = Reynolds number, $(d\,U_{avg}\rho/\mu)$
N_{Sc} = Schmidt number, $(\mu/\rho D)$

Greek Letters

α = solution rate constant, (L/θ)
Δ = difference
κ = Boltzman constant, $(1.38 \times 10^{-16}$ erg. °K.)
μ = viscosity, (g./cm. sec.) $(m/L\theta)$
ρ = density, (M/L^3)
ϕ_D = defined by Equation (6)

Subscripts

C = cross sectional
D = deposition
m = mean value
o = wall value
P = peripheral
S = solution
f = filter outlet value

Superscripts

° = equilibrium value

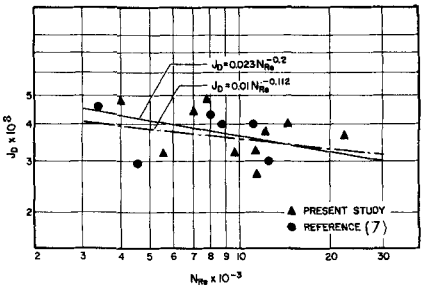

Fig. 4. Correlation of mass transfer coefficients.

LITERATURE CITED

1. Bagley, K. Q., and K. R. Montgomery, United Kingdom Atomic Energy Authority, *Rep. No. IGR-TN/C 250.*
2. Boelter, L. M. K., R. C. Martinelli, and Finn Jonassen, *Trans. Am. Soc. Mech. Engrs.*, **63**, 447 (1941).
3. Bychkov, Y. F., A. N. Rosanov, and V. B. Yakolev, *Atomnaya Energiya*, **7**, No. 6 (1959).
4. Chilton, T. H., and A. P. Colburn, *Ind. Eng. Chem.*, **26**, 1183 (1934).
5. Deissler, R. G., *Natl. Advisory Comm. Aeronaut., Rep. 1210* (1955).
6. *Ibid., Tech. Note 2138* (1950).
7. Dunn, W. E., C. F. Bonilla, C. Ferstenberg, and B. Gross, *A.I.Ch.E. Journal*, **2**, 184 (1956).
8. Epstein, L. F., *Chem. Eng. Progr. Symposium Ser. No. 20*, **53**, 67 (1957).
9. Friend, W. L., and A. B. Metzner, *A.I.Ch.E. Journal*, **4**, 393 (1958).
10. Gill, W. N., R. P. Vanek, R. V. Jelinek, and C. S. Grove, Jr., *A.I.Ch.E. Journal*, **6**, 139 (1960).
11. Hoffman, E. E., and L. R. Trotter, "Corrosion and Mass Transfer by Lithium at Elevated Temperatures," Metallurgy Information Meeting, Iowa State College, Ames, Iowa (May, 1956).
12. Horsley, G. W., *J. Nucl. Energy, Part B*, **1**, 84 (1959).
13. Leavenworth, H. W., A. W. Smith, and R. E. Cleary, A.C.S. Meeting, Univ. Mass., Amherst (Nov., 1959).
14. Lin, C. S., R. W. Moulton, and G. L. Putnam, *Ind. Eng. Chem.*, **45**, 636 (1953).
15. Linton, W. H., Jr., and T. K. Sherwood, *Chem. Eng. Progr.*, **46**, 258 (1950).
16. McLean, D., "Grain Boundaries in Metals," Clarendon Press, Oxford (1957).
17. Sherwood, T. K., and R. L. Pigford, "Absorption and Extraction," McGraw-Hill, New York (1952).
18. Sand, J. J., W. N. Gill, R. V. Jelinek, and C. S. Grove, paper presented at A.I.Ch.E. Meeting, Kansas City (1959).
19. Strauss, S. W., J. L. White, and B. F. Brown, *Acta Metallurgica*, **9**, 604 (1958).

Manuscript received April 27, 1960; revision received October 3, 1960; paper accepted October 5, 1960.